Rodded Depletion Analysis of Soluble Boron-Free SMR Using Axially-shielded Burnable Absorber (ABA) in the Equilibrium Cycle

Yunseok Jeong [a], Jaehyun Ryu [a], and Yonghee Kim [a*]
[a]*Nuclear and Quantum Engineering, KAIST*
[*]*Corresponding author: yongheekim@kaist.ac.kr*

Keywords : Axially-shielded burnable absorber, soluble boron-free, SMR, rodded depletion, axial shape index

1. Introduction

Soluble boron-free (SBF) SMRs can simplify the reactor system, improve inherent safety, and enhance load-follow capability, but the large excess reactivity must then be controlled almost entirely by burnable absorbers (BAs). Conventional BAs such as integral gadolinia burnable absorbers (IGD), IFBA, and WABA suffer under SBF conditions from rapid absorber depletion and reactivity upswing, reduced fuel inventory, or interference with control rod utilization, while advanced BA concepts [1-3] often require new fabrication methods or face licensing challenges.

To address this need, the axially-shielded burnable absorber (ABA) was proposed as a practical BA concept based on conventional IGD technology. Its neutronic feasibility was demonstrated in the initial cycle of an SBF SMR [4], and the concept was extended to the equilibrium cycle under unrodded, equilibrium-xenon conditions [5]; the overall development is documented in the author's Ph.D. dissertation [6].

However, the previous equilibrium-cycle evaluation was limited to all-rods-out (ARO) conditions, and the tertiary burnable absorber (TBA) regions placed at the top and bottom of the fuel column induced an alternating axial power skew between successive cycles. In this study, the equilibrium cycle is analyzed under rodded critical depletion, with an alternative Zone 1 configuration in which the TBA bands are relocated to the mid-column positions [6] to facilitate axial power distribution control.

2. Methods

2.1 Core Model

The present study considered a soluble boron-free SMR core whose basic specifications were referenced from the iSMR design [3]. Whole-core depletion calculations were performed with the continuous-energy Monte Carlo code Serpent 2 [7] for the equilibrium cycle under both ARO and rodded critical conditions.

2.2 ABA Design Concept

The axially-shielded burnable absorber (ABA) forms axially localized IGD regions by loading one or multiple consecutive IGD pellets between standard UO_2 pellet regions, so that the absorber depletion is controlled through axial self-shielding [4]. The IGD regions are classified into primary, secondary, and tertiary burnable absorber (PBA, SBA, and TBA) zones with different gadolinia contents, so that their depletion timings are staged over the cycle: the PBA remains effective until near EOC, the SBA suppresses early- and mid-cycle excess reactivity, and the TBA suppresses the initial excess reactivity [4,6]. The U-235 enrichment of the IGD pellets was adjusted according to Eq. (1) to compensate for the degraded thermal conductivity of the UO_2-Gd_2O_3 pellet.

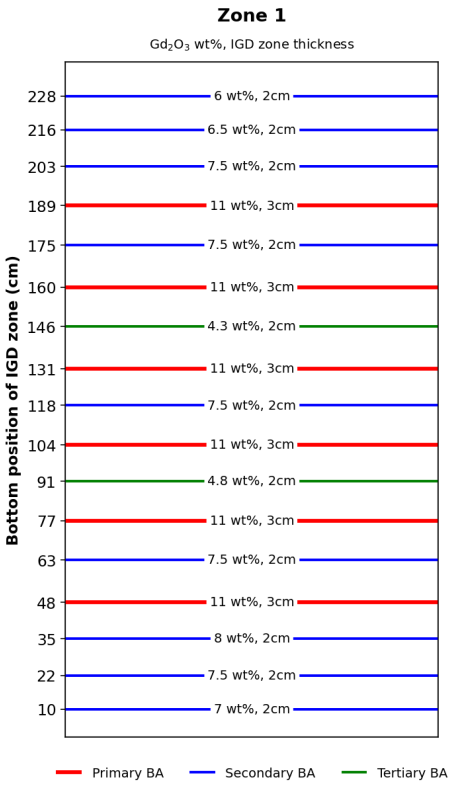
$$4.65 \times (1 - 0.05 \times wt\%) \quad (1)$$

2.3 ABA Configuration for the Equilibrium Cycle

In the equilibrium cycle, all fresh fuel assemblies employ 4.95 wt% U-235 enrichment, and a larger BA inventory is required than in the initial cycle. Two ABA assembly types were employed: Zone 1 for inner-core positions, where the higher neutron flux demands stronger reactivity suppression, and Zone 2 for outer-core positions. Erbia was additionally doped into the standard UO_2 pellets of Zone 1, 0.15 wt% for the upper five standard fuel regions and 0.30 wt% for the lower regions, to provide finer reactivity control [6]. 2 cm-thick IGD regions were used as the basic configuration, while the PBA regions of Zone 1 employed 3 cm-thick IGD regions for the lower initial reactivity required near the core center.

In contrast to the previous equilibrium core [5], in which the TBA bands of Zone 1 were placed at the fuel column ends, the present design relocates them to the mid-column positions, while the column-end bands are replaced by SBA with a relatively high gadolinia content [6]. An absorber at the axial extremity promotes axial power skewness, since its gadolinium depletion raises the local power and thereby accelerates the remaining depletion; relocating the weakly shielded TBA to the mid-column weakens this feedback. The axial configurations of both assembly types are shown in

Figure 1, with Zone 2 unchanged from the previous core [5].



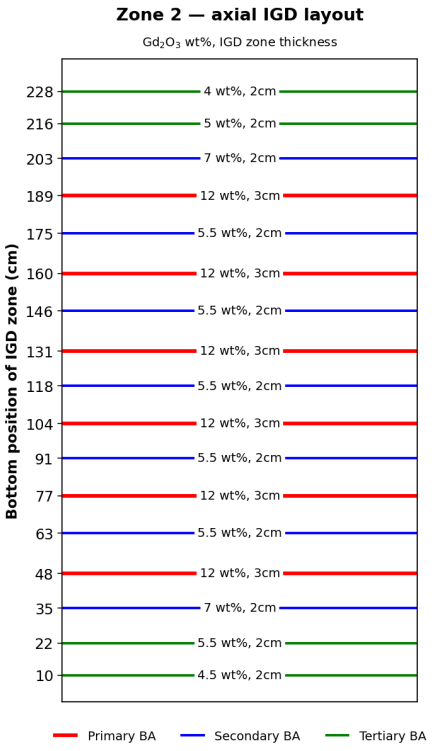


Figure 1 Axial configuration of the ABA fuel assemblies (Zones 1 and 2) in the equilibrium cycle

2.4 Fuel Shuffling Scheme

A multi-batch fuel management scheme was adopted to establish the equilibrium cycle, as shown in Figure 2. In each cycle, 35 out of 69 fuel assemblies are reloaded, while the others are shuffled according to a predetermined radial loading pattern. The central assembly is burned and discharged every cycle, and the same assembly design as that used at the core center in the initial cycle was adopted for this position.

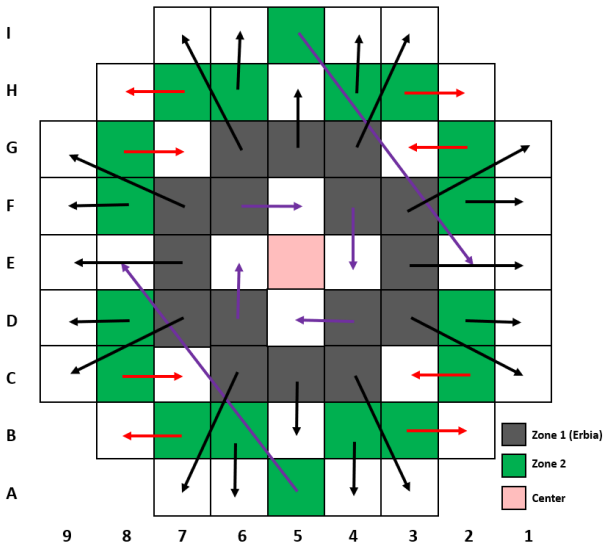


Figure 2 Fuel loading and shuffling pattern of the equilibrium core

2.5 Control Rod Pattern and Specifications

The control rod system consists of two gray banks (GR1 and GR2), three regulating banks (RB1, RB2, and RB3), and one shutdown bank (SB). GR2 employs a hafnium rod of 0.25 cm radius clad in Inconel-625 for cycle reactivity control, while GR1 employs an Inconel-625 rod so that its per-assembly worth is smaller and finer reactivity control is possible. The regulating banks use natural B_4C, and the shutdown bank uses 95 wt% enriched B_4C to ensure the shutdown margin, as summarized in Table 1.

The bank insertion sequence is GR2 first, followed by GR1 and then the regulating banks, with no overlap between GR2 and GR1. The control rod pattern is shown in Figure 3.

Table 1 Control rod materials

Bank	Material
GR2	Inconel-625 cladded Hf (Hf 0.25 cm)
GR1	Inconel-625
RB1, RB2, RB3	Natural B_4C

SB 95 wt% enriched B_4C

Y/X	5	4	3	2	1
E	GR2	SB	RB3	SB	SB
D	SB	RB2		RB1	SB
C	RB3		GR1	SB	
B	SB	RB1	SB	SB	
A	SB	SB			

Figure 3 Control rod pattern (quarter core)

3. Numerical Results

The depletion calculations used 150,000 particles with 100 inactive and 200 active cycles under equilibrium xenon conditions. The fuel temperature was fixed at 903.15 K, and the coolant temperature was linearly interpolated along the axial direction between the inlet and outlet temperatures. The rodded results were obtained from a burnup-dependent critical rod search following the insertion sequence of Section 2.5.

3.1 ARO Reactivity Curve

Figure 4 shows the ARO reactivity curves for the even and odd cycles, which alternate in pairs in the converged equilibrium state. The BOC reactivity is approximately 900 pcm; it decreases to a minimum of approximately 280 pcm near 250 EFPD, rises to a mid-cycle maximum of approximately 840 pcm near 550 EFPD, and becomes slightly negative shortly before 800 EFPD. The excess reactivity thus remains below 1,000 pcm and is small enough to be covered by the gray banks. The minimum of approximately 280 pcm, however, leaves a limited operational margin once nuclear-data and computational uncertainties and the xenon buildup accompanying load-follow operation are considered; a follow-up study to raise the minimum excess reactivity is in progress.

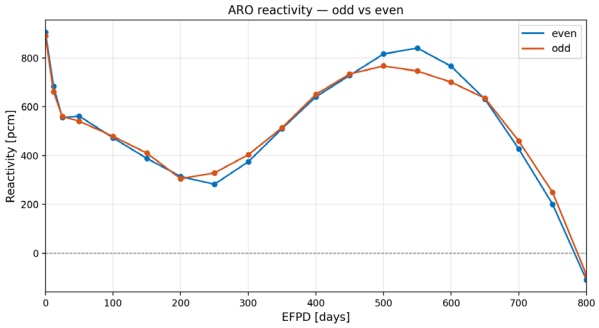


Figure 4 ARO reactivity curves of the equilibrium cycle (even and odd cycles)

3.2 Rodded Depletion Results

Figure 5 shows the critical rod positions and the ASI over the equilibrium cycle. GR2 remains fully inserted over most of the cycle, while GR1 moves between approximately 16% and 100% of the core height to follow the cycle reactivity variation, being fully withdrawn near 250 EFPD where the excess reactivity is minimum. Although the ARO reactivity becomes slightly negative before 800 EFPD, criticality is maintained up to 800 EFPD in the rodded depletion, whose burnup history differs from the ARO case, so that the full 800-EFPD cycle length is achievable in rodded operation. The ASI remains within ±0.13, and the corresponding axial power distributions are shown in Figure 6: the axial peaking factor F_z is 1.33 at BOC, 1.42 at MOC, and 1.24 at EOC in the even cycle, with nearly identical odd-cycle values.

The radial and total power peaking factors are shown in Figure 7. The radial peaking factor F_r varies between approximately 1.36 and 1.63, increasing toward EOC, and the total peaking factor F_q reaches a maximum of approximately 2.31, below the design acceptance limit of 2.43. The 1-sigma statistical uncertainty of F_q, which reflects the local power peaks formed around the axially discontinuous IGD regions, is approximately 2%, and the maximum remains below the limit even with this uncertainty.

The radial assembly power distributions at BOC, MOC, and EOC are shown in Figure 8 for the even cycle, in terms of assembly-wise normalized powers that exclude the intra-assembly pin peaking factor; the even-odd difference is negligible. The assembly-wise radial peaking increases from 1.33 at BOC to 1.38 at MOC and 1.52 at EOC, because the residual burnable absorber of the inner Zone 1 assemblies depletes late in the cycle and the local power of that region rises accordingly.

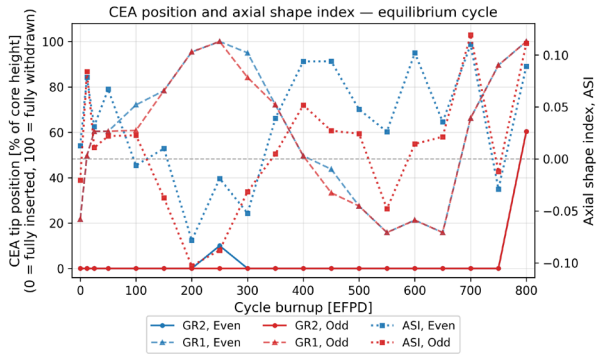


Figure 5 Critical rod positions and ASI over the equilibrium cycle (even and odd cycles)

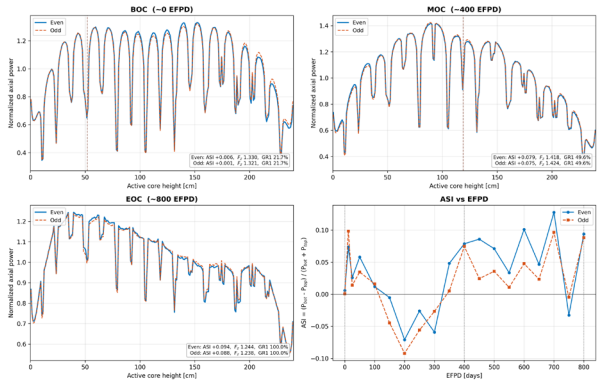


Figure 6 Axial power distributions at BOC, MOC, and EOC and ASI over the equilibrium cycle (even and odd cycles)

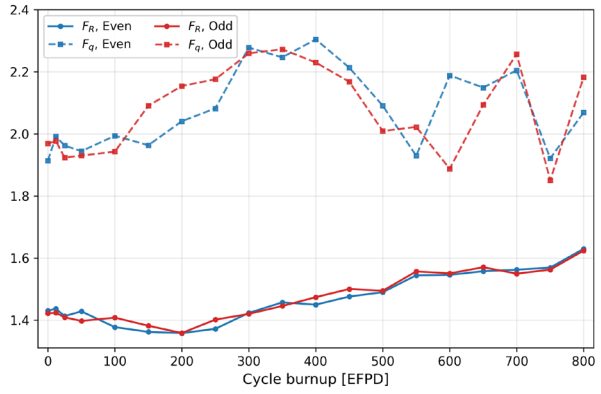


Figure 7 Radial and total power peaking factors over the equilibrium cycle

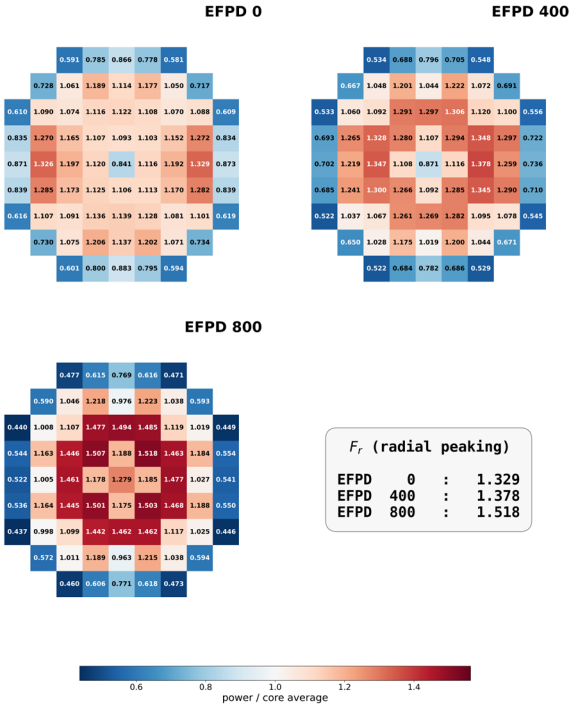


Figure 8 Radial assembly power distributions at BOC, MOC, and EOC (even cycle)

3.3 Fuel Discharge Burnup

Figure 9 shows the assembly-wise discharge burnup distribution for the even cycle; the even-odd difference is negligible. The average discharge burnup is 40.1 GWd/tU including the center assembly and 40.7 GWd/tU excluding it, with a maximum of 48.9 GWd/tU, while the single-cycle center assembly is discharged at 17.6 GWd/tU.

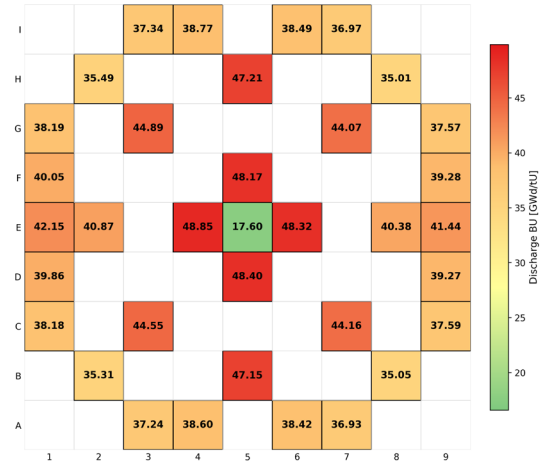


Figure 9 Assembly-wise discharge burnup distribution (even cycle)

4. Conclusions

The ABA-loaded equilibrium core of a soluble boron-

free SMR was evaluated under rodded critical depletion, with the Zone 1 TBA bands relocated from the fuel column ends to the mid-column positions.

The ARO excess reactivity stays below 1,000 pcm over the cycle, with a BOC value of approximately 900 pcm and a mid-cycle maximum of approximately 840 pcm. Criticality is maintained over the full 800-EFPD cycle under rodded operation, with the ASI within ±0.13, an axial peaking factor below 1.42, and a maximum F_q of approximately 2.31 below the 2.43 limit. The average discharge burnup is 40.1 GWd/tU including the center assembly and 40.7 GWd/tU excluding it. The axial staging of the burnable absorber is therefore a practical means of controlling the axial power distribution in the equilibrium cycle, while raising the minimum excess reactivity remains as future work.

REFERENCES

1. X. H. Nguyen, C. H. Kim, and Y. H. Kim, "An advanced core design for a soluble-boron-free small modular reactor ATOM with centrally-shielded burnable absorber," Nuclear Engineering and Technology, vol. 51, no. 2, pp. 369–376, Feb. 2019, doi: 10.1016/j.net.2018.11.016.
2. S. Wijaya, X. H. Nguyen, Y. Jeong, and Y. H. Kim, "Multi-batch core design study for innovative small modular reactor based on centrally-shielded burnable absorber," Nuclear Engineering and Technology, vol. 56, no. 3, pp. 907–915, Mar. 2024, doi: 10.1016/j.net.2023.11.007.
3. J. S. Kim, et al., "Highly Intensive Gadolinium/Alumina (HIGA) burnable absorber rods for soluble-boron-free i-SMR core," *Transactions of the Korean Nuclear Society Spring Meeting*, 2024.
4. Y. Jeong, J. Ryu, D. Choi, Y. Lee, and Y. Kim, "Axially-shielded Burnable Absorber (ABA) for Soluble Boron-Free SMR: Neutronics Feasibility in the Initial Cycle," *Transactions of the Korean Nuclear Society Autumn Meeting*, October 30-31, 2025.
5. Y. Jeong, J. Ryu, and Y. Kim, "Neutronics Performance of Axially-shielded Burnable Absorber (ABA) in the Equilibrium Cycle of Soluble Boron-Free SMR," *Transactions of the Korean Nuclear Society Spring Meeting*, May 7-8, 2026.
6. Y. Jeong, "A Novel Axially-shielded Burnable Absorber (ABA) Development for Soluble Boron-Free Small Modular Reactor," Ph.D. Dissertation, KAIST, 2026.
7. J. Leppänen, M. Pusa, T. Viitanen, V. Valtavirta, and T. Kaltiaisenaho, "The Serpent Monte Carlo code: Status, development and applications in 2013," Annals of Nuclear Energy, vol. 82, pp. 142–150, Aug. 2015, doi: 10.1016/j.anucene.2014.08.024.